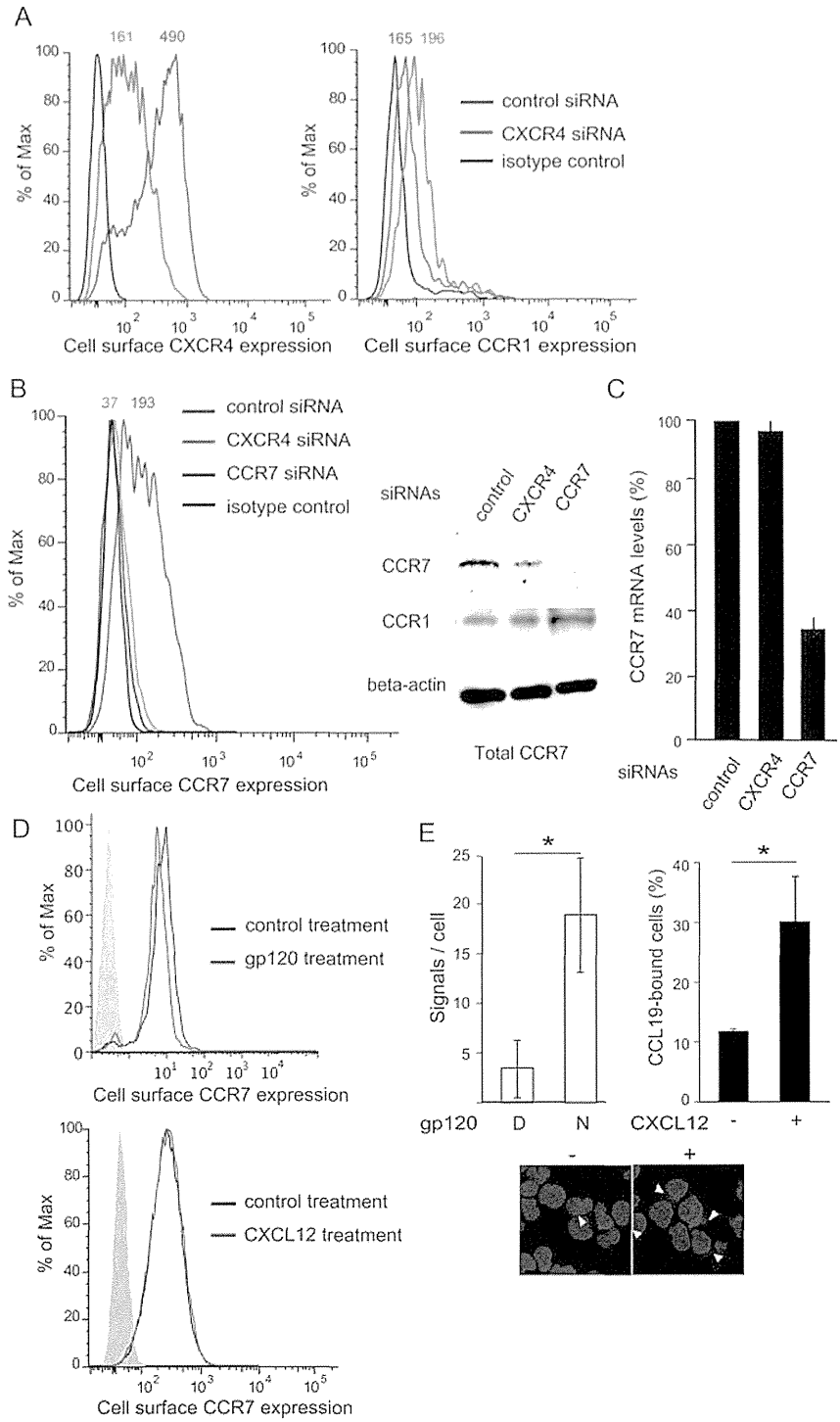

Fig 6. CXCR4 is required for stable CCR7 expression, CCR7 ligand binding, and CCR7 homo-oligomer formation. (A) The cell surface expression levels of CXCR4 and CCR1 were evaluated by flow cytometry using anti-CXCR4 (left) or anti-CCR1 (right) antibodies in control or CXCR4 siRNA-treated H9 cells. Mean fluorescence intensity is indicated on the histograms. (B) The cell surface CCR7 expression was evaluated by flow cytometry using anti-CCR7 antibody. H9 cells treated with control, CXCR4, or CCR7 siRNAs were analyzed (left). The total cellular CCR7 and CCR1 expression levels in control, CXCR4, or CCR7 siRNA-treated H9 cells were analyzed by Western blotting. Anti-β actin mAb was used to confirm equal loading (right). (C) The *CCR7* mRNA expression levels were analyzed in control, CXCR4, or CCR7 siRNA-treated H9 cells by quantitative RT-PCR. (D) The cell surface CCR7 expression levels were analyzed

in gp120-treated human CD4 T cells (upper panel), and CXCL12-treated H9 cells (lower panel) by flow cytometry. (E) The CCR7 ligand-binding abilities in H9 cells pretreated with a native (N) or control, heat-denatured gp120 (D), or with (+) or without (–) 100 ng/ml CXCL12 were examined by CCL19-Ig binding. A minimum of three images per section was observed by confocal microscopy, and the relative fluorescence signal or the percentage of CCL19-Ig bound cells was quantified using Duolink Image Tool software. The images of CCL19-bound cells with or without CXCL12 pretreatment are shown in the right panel (indicated by white triangles). *, $p < 0.05$, Student's *t*-test.

doi:10.1371/journal.pone.0117454.g006

oligomerization (Fig. 7F). These results suggest that CXCR4 ligand-induced signaling promotes CXCR4/CCR7 hetero-oligomerization in CD4 T cells.

Discussion

CXCR4 binding molecules stimulate CCR7-dependent CD4 T cell responses

In this study, we demonstrated that the recombinant X4-HIV-1_{NL4-3}-derived gp120 enabled human CD4 T cells to respond to minimum concentrations of CCL21 or CCL19, suggesting that HIV-1 gp120 cooperated with CCR7 ligands to enhance CD4 T cell migration. Our results are partly consistent with those reported by Green et al. [19], who demonstrated that X4-HIV-1_{IIIB}-derived gp120 promoted CCL21-dependent CD4 T cell migration. However, whereas they found that gp120 cooperates with CCL21 but not with another CCR7 ligand, CCL19, we observed effective cooperation for both CCR7 ligands. This discrepancy may be due to the different sources of gp120 preparation between studies, which may influence the affinity of gp120 for CXCR4.

Requirement of CXCR4 and CD4 for the enhancing effect of gp120

As the X4 gp120 can interact directly with CXCR4 independently of CD4 [27], [28] and mimics the effects of CXCL12 in cellular responses via CXCR4 [3], [4], [29], we speculated that gp120 directly exerts its enhancing effects via CXCR4. Accordingly, we found that gp120's promoting effect was inhibited almost to the basal level in the presence of a neutralizing anti-CXCR4 antibody *in vitro* (Fig. 2B), whereas the effect of HIV-1 gp120 was inhibited by sCD4 to a lesser extent. This result supports the idea that X4 gp120 acts primarily through CXCR4 to promote CCR7-dependent cell migration and that the interaction between gp120 and CD4 may be less important in this process. However, considering that HIV-1 gp120 activates multiple CD4-mediated intracellular signaling pathways, such as T cell apoptosis [30], mitogen-activated protein kinase pathways [2], and chemokine receptor down-regulation [31], [32], gp120 binding to CD4 may also play a role in enhancement of CCR7-dependent T cell trafficking *in vivo*.

A possible mechanism of CXCR4-mediated CCR7 sensitization

Our current and previous data [18] have shown that neither CXCL12 nor gp120 significantly increased cell surface CCR7 expression, suggesting that CXCR4 signaling increases CCR7 ligand binding through a mechanism other than the quantitative change in CCR7 receptor expression on the T cell surface. Recently, several reports have shown that oligomerization of chemokine receptors is involved in their functional activation, ligand binding, and induction of specific signaling cascades [25]. We found that CCR7 constitutively formed homo-oligomers at basal levels in the absence of CCR7 or CXCR4 ligands, and that this homo-oligomerization was significantly enhanced after CXCR4 signaling. We also found that CCR7 constitutively forms heterodimers with CXCR4, which was promoted subsequent to CXCR4 ligand stimulation. The observed formation of homo- and hetero-oligomers raises questions as to whether these

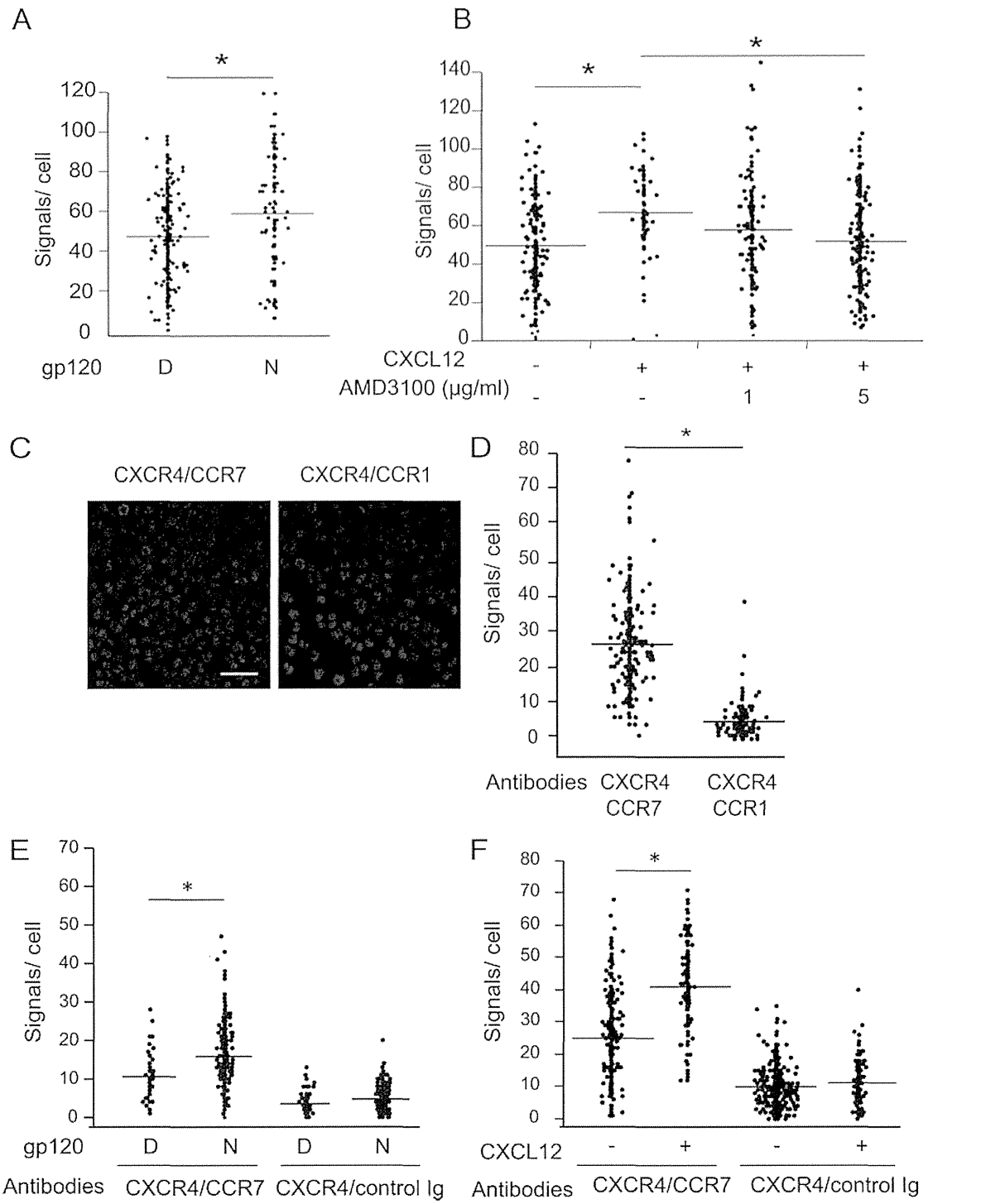

Fig 7. CXCR4 ligand binding facilitates CXCR4/CCR7 hetero-oligomer formation. (A) CCR7 homo-oligomer formation in H9 cells after treatment with or without 1 μg/ml recombinant gp120 was examined by *in situ* PLA. The number of *in situ* PLA signals per cell was counted by using the Duolink Image Tool software. The result shown is a representative result from three independent experiments showing the mean number of the signals plotted on the vertical axis. *, $p < 0.05$ by Mann-Whitney's U test. (B) CCR7 homo-oligomer formation in H9 cells after treatment with 100 ng/ml CXCL12 was examined, as described in (A). Quantification of CCR7 homo-oligomers after CXCL12 pretreatment in the presence or absence of 1 or 5 μg/ml AMD3100. The result shown is a representative result from five independent experiments. *, $p < 0.05$ by Mann-Whitney's U test. (C) CXCR4/CCR7 or CXCR4/CCR1 hetero-oligomer formation in H9 cells by *in situ* PLA using the indicated combinations of antibodies. The z-stack images derived from sections covering 10 μm with a 0.5-μm step are shown. Scale bar represents 50 μm. (D) Quantification of the detected *in situ* PLA signals per cell was performed. The result shown is a representative result from three independent experiments. *, $p < 0.05$ by Mann-Whitney's U test. (E) CXCR4/CCR7 hetero-oligomer formation in H9 cells after treatment with 1 μg/ml

gp120 in a native form (N) or control heat-denatured form (D) was examined by the PLA using the indicated combinations of antibodies. (F) CXCR4/CCR7 hetero-oligomer formation was examined with 100 ng/ml CXCL12 as described in (E).

doi:10.1371/journal.pone.0117454.g007

complexes play a functional role in the up-regulation of CCR7-dependent signaling by CXCR4 ligands. We speculate that induction of CCR7 homo-oligomerization is coupled to direct receptor activation, as some chemokine receptors are activated through receptor dimerization upon ligand binding; for example, CXCL12-induced CXCR4 dimerization activates CXCR4's downstream signaling pathway [33]. In addition, ligand-dependent CCR2 dimerization was observed with the monocyte chemoattractant protein-1 receptor, CCR2, and this dimerization was shown to be functionally relevant in the ligand-induced signal transduction pathway [34]. It is also likely that CXCR4/CCR7 hetero-oligomerization may directly and/or indirectly modulate CCR7 responses; that is, ligand binding to CXCR4 may influence the conformational state, ligand binding affinity, and assembly of signaling complexes to CCR7. Indeed, there are several reports demonstrating the importance of chemokine receptor cross-communication for signal amplification and diversification; CCR2/CCR5 hetero-oligomerization increases the receptor sensitivity to chemokine ligands and triggers distinct signaling pathways [35]. CXCR7/CXCR4 heterodimerization has been shown to alter CXCR4-mediated G-protein-coupled signaling [36] and preferentially activates the alternative β-arrestin-linked signaling pathway [37]. In addition, we speculate that ligand-independent CXCR4/CCR7 oligomerization may contribute to maintaining the functional CCR7 level, which is supported by the results of our siRNA knockdown experiments showing that CXCR4 contributes to stable CCR7 expression on the plasma membrane. To verify the involvement of these receptor oligomerizations in regulating CCR7-ligand responsiveness, we are currently adopting an experimental approach previously reported [38], [39] to disrupt CXCR4 or CCR5 oligomers with synthetic peptides that can destabilize chemokine receptor oligomerization.

Possible contribution of gp120 to CD4 T cell trafficking *in vivo*

Whereas Green et al. [19] also demonstrated that gp120-sensitized lymphocytes migrated to LNs in a CCR7-dependent manner, this result was observed following intravenous injection of lymphocytes in immunocompromised NOD-SCID mice. In contrast, we demonstrated the gp120-induced promotion of CD4 T cell migration upon injection of lymphocytes into the footpads of normal mice, because the lymphatics are considered to be an important route for the systemic spread of HIV-infected T cells [40] [41]. Thus, we suggest that HIV gp120 contributes to both the hematogenous and lymphatic spread of CD4 T cells. These data indicate that inhibition of gp120 activity may help to normalize T cell trafficking, which may in turn help to restore immunocompetence in HIV-infected patients.

It has been reported previously that CD4 T cells are sequestered in lymphoid tissues and then reappear in the blood after active antiretroviral therapy in HIV-infected patients [42], implying that the CD4 T cell distribution can be regulated by certain signals from the virus itself. Although the mechanistic basis for this phenomenon remains unclear, our findings that gp120 promotes CCR7-dependent T cell migration in a CXCR4-dependent manner shed some light in this regard.

In our previous study using mouse T cells, CXCL12 concentrations of 250 nM or higher were required to observe a synergistic effect on CCR7-dependent migration *in vitro* [18], whereas in this study, HIV gp120 concentrations of only 170 nM or greater were required to observe the enhancing effect on primary human CD4 T cells. From these results, we speculate that nanomolar concentrations of CXCR4-binding molecules would be required for generating a synergistic effect on CCR7-dependent cell migration. Although there is currently no accurate

information related to the CXCL12 and gp120 concentrations in local tissues, the reported plasma level of CXCL12 is ~200 pM [43] and the concentrations of gp120 in HIV-infected patients' sera vary from 2 to 800 pM depending on sample preparation and quantifying methods [44], which are much lower levels than those used in our *in vitro* experiments. On the other hand, the CXCR4 ligand concentrations in specific tissue microenvironments are speculated to be in the micromolar range because CXCL12 strongly binds to tissue matrix components, including glycosaminoglycans/proteoglycans [45], and gp120 is also captured by matrix components [46] or dendritic cells [47]. In addition, the finding that CXCL12 functions more effectively when in immobilized form than soluble form [48] supports the idea that CXCR4 ligands can be presented at functional concentrations to promote CCR7-dependent T cell migration *in vivo*. The specific biological role of soluble and/or matrix-associated CXCR4 ligands in controlling CCR7-dependent CD4 T cell trafficking is an important topic for further research in understanding the role of CD4 T cell migration in HIV-1 pathogenesis.

Acknowledgments

We would like to express our appreciation to Dr. N. Sasaki, Dr. E. Umemoto, Ms. E. Hata (Osaka University), and Dr. I. Shimada (The University of Tokyo) for helpful suggestions. We thank Ms. Y. Wakabayashi and N. Yoshizumi for technical assistance. We thank Ms. S. Yamashita for secretarial assistance.

Author Contributions

Conceived and designed the experiments: HH TS MM. Performed the experiments: HH DK HY EEN. Analyzed the data: HH DK HY. Contributed reagents/materials/analysis tools: HH DK HY EEN. Wrote the paper: HH MM.

References

1. Freedman BD, Liu QH, Del Corno M, Collman RG (2003) HIV-1 gp120 chemokine receptor-mediated signaling in human macrophages. Immunol Res 27: 261–276. PMID: 12857973
2. Lee C, Liu QH, Tomkowicz B, Yi Y, Freedman BD, et al. (2003) Macrophage activation through CCR5- and CXCR4-mediated gp120-elicited signaling pathways. J Leukoc Biol 74: 676–682. PMID: 12960231
3. Balabanian K, Harriague J, Decrion C, Lagane B, Shorte S, et al. (2004) CXCR4-tropic HIV-1 envelope glycoprotein functions as a viral chemokine in unstimulated primary $CD4^+$ T lymphocytes. J Immunol 173: 7150–7160. PMID: 15585836
4. Iyengar S, Schwartz DH, Hildreth JE (1999) T cell-tropic HIV gp120 mediates CD4 and CD8 cell chemotaxis through CXCR4 independent of CD4: implications for HIV pathogenesis. J Immunol 162: 6263–6267. PMID: 10229873
5. von Andrian UH, Mempel TR (2003) Homing and cellular traffic in lymph nodes. Nat Rev Immunol 3: 867–878. PMID: 14668803
6. Miyasaka M, Tanaka T (2004) Lymphocyte trafficking across high endothelial venules: dogmas and enigmas. Nat Rev Immunol 4: 360–370. PMID: 15122201
7. Campbell JJ, Bowman EP, Murphy K, Youngman KR, Siani MA, et al. (1998) 6-C-kine (SLC), a lymphocyte adhesion-triggering chemokine expressed by high endothelium, is an agonist for the MIP-3β receptor CCR7. J Cell Biol 141: 1053–1059. PMID: 9585422
8. Yoshida R, Nagira M, Imai T, Baba M, Takagi S, et al. (1998) EBI1-ligand chemokine (ELC) attracts a broad spectrum of lymphocytes: activated T cells strongly up-regulate CCR7 and efficiently migrate toward ELC. Int Immunol 10: 901–910. PMID: 9701028
9. Nagasawa T, Tachibana K, Kishimoto T (1998) A novel CXC chemokine PBSF/SDF-1 and its receptor CXCR4: their functions in development, hematopoiesis and HIV infection. Semin Immunol 10: 179–185. PMID: 9653044

10. Legler DF, Loetscher M, Roos RS, Clark-Lewis I, Baggiolini M, et al. (1998) B cell-attracting chemokine 1, a human CXC chemokine expressed in lymphoid tissues, selectively attracts B lymphocytes via BLR1/CXCR5. J Exp Med 187: 655–660. PMID: 9463416

11. Ebisuno Y, Tanaka T, Kanemitsu N, Kanda H, Yamaguchi K, et al. (2003) Cutting edge: the B cell chemokine CXC chemokine ligand 13/B lymphocyte chemoattractant is expressed in the high endothelial venules of lymph nodes and Peyer's patches and affects B cell trafficking across high endothelial venules. J Immunol 171: 1642–1646. PMID: 12902460

12. Kanemitsu N, Ebisuno Y, Tanaka T, Otani K, Hayasaka H, et al. (2005) CXCL13 is an arrest chemokine for B cells in high endothelial venules. Blood 106: 2613–2618. PMID: 15972452

13. Yang BG, Tanaka T, Jang MH, Bai Z, Hayasaka H, et al. (2007) Binding of lymphoid chemokines to collagen IV that accumulates in the basal lamina of high endothelial venules: its implications in lymphocyte trafficking. J Immunol 179: 4376–4382. PMID: 17878332

14. Paoletti S, Petkovic V, Sebastiani S, Danelon MG, Uguccioni M, et al. (2005) A rich chemokine environment strongly enhances leukocyte migration and activities. Blood 105: 3405–3412. PMID: 15546958

15. Contento RL, Molon B, Boularan C, Pozzan T, Manes S, et al. (2008) CXCR4-CCR5: a couple modulating T cell functions. Proc Natl Acad Sci U S A 105: 10101–10106. doi: 10.1073/pnas.0804286105 PMID: 18632580

16. Vanbervliet B, Bendriss-Vermare N, Massacrier C, Homey B, de Bouteiller O, et al. (2003) The inducible CXCR3 ligands control plasmacytoid dendritic cell responsiveness to the constitutive chemokine stromal cell-derived factor 1 (SDF-1)/CXCL12. J Exp Med 198: 823–830. PMID: 12953097

17. Umemoto E, Otani K, Ikeno T, Verjan Garcia N, Hayasaka H, et al. (2012) Constitutive plasmacytoid dendritic cell migration to the splenic white pulp is cooperatively regulated by CCR7- and CXCR4-mediated signaling. J Immunol 189: 191–199. doi: 10.4049/jimmunol.1200802 PMID: 22634622

18. Bai Z, Hayasaka H, Kobayashi M, Li W, Guo Z, et al. (2009) CXC chemokine ligand 12 promotes CCR7-dependent naive T cell trafficking to lymph nodes and Peyer's patches. J Immunol 182: 1287–1295. PMID: 19155474

19. Green DS, Center DM, Cruikshank WW (2009) Human immunodeficiency virus type 1 gp120 reprogramming of $CD4^+$ T-cell migration provides a mechanism for lymphadenopathy. J Virol 83: 5765–5772. doi: 10.1128/JVI.00130-09 PMID: 19297493

20. Yu D, Shioda T, Kato A, Hasan MK, Sakai Y, et al. (1997) Sendai virus-based expression of HIV-1 gp120: reinforcement by the V(-) version. Genes Cells 2: 457–466. PMID: 9366551

21. Ohishi M, Shioda T, Sakuragi J (2007) Retro-transduction by virus pseudotyped with glycoprotein of vesicular stomatitis virus. Virology 362: 131–138. PMID: 17258261

22. Nitta N, Tsuchiya T, Yamauchi A, Tamatani T, Kanegasaki S (2007) Quantitative analysis of eosinophil chemotaxis tracked using a novel optical device—TAXIScan. J Immunol Methods 320: 155–163. PMID: 17289072

23. Lapham CK, Ouyang J, Chandrasekhar B, Nguyen NY, Dimitrov DS, et al. (1996) Evidence for cell-surface association between fusin and the CD4-gp120 complex in human cell lines. Science 274: 602–605. PMID: 8849450

24. Debes GF, Arnold CN, Young AJ, Krautwald S, Lipp M, et al. (2005) Chemokine receptor CCR7 required for T lymphocyte exit from peripheral tissues. Nat Immunol 6: 889–894. PMID: 16116468

25. Munoz LM, Holgado BL, Martinez AC, Rodriguez-Frade JM, Mellado M (2012) Chemokine receptor oligomerization: a further step toward chemokine function. Immunol Lett 145: 23–29. doi: 10.1016/j.imlet.2012.04.012 PMID: 22698180

26. Soderberg O, Leuchowius KJ, Gullberg M, Jarvius M, Weibrecht I, et al. (2008) Characterizing proteins and their interactions in cells and tissues using the in situ proximity ligation assay. Methods 45: 227–232. doi: 10.1016/j.ymeth.2008.06.014 PMID: 18620061

27. Bandres JC, Wang QF, O'Leary J, Baleaux F, Amara A, et al. (1998) Human immunodeficiency virus (HIV) envelope binds to CXCR4 independently of CD4, and binding can be enhanced by interaction with soluble CD4 or by HIV envelope deglycosylation. J Virol 72: 2500–2504. PMID: 9499113

28. Misse D, Cerutti M, Schmidt I, Jansen A, Devauchelle G, et al. (1998) Dissociation of the CD4 and CXCR4 binding properties of human immunodeficiency virus type 1 gp120 by deletion of the first putative α-helical conserved structure. J Virol 72: 7280–7288. PMID: 9696823

29. Misse D, Cerutti M, Noraz N, Jourdan P, Favero J, et al. (1999) A CD4-independent interaction of human immunodeficiency virus-1 gp120 with CXCR4 induces their cointernalization, cell signaling, and T-cell chemotaxis. Blood 93: 2454–2462. PMID: 10194422

30. Banda NK, Bernier J, Kurahara DK, Kurrle R, Haigwood N, et al. (1992) Crosslinking CD4 by human immunodeficiency virus gp120 primes T cells for activation-induced apoptosis. J Exp Med 176: 1099–1106. PMID: 1402655

31. Su SB, Gong W, Grimm M, Utsunomiya I, Sargeant R, et al. (1999) Inhibition of tyrosine kinase activation blocks the down-regulation of CXC chemokine receptor 4 by HIV-1 gp120 in CD4+ T cells. J Immunol 162: 7128–7132. PMID: 10358157

32. Wang JM, Ueda H, Howard OM, Grimm MC, Chertov O, et al. (1998) HIV-1 envelope gp120 inhibits the monocyte response to chemokines through CD4 signal-dependent chemokine receptor down-regulation. J Immunol 161: 4309–4317. PMID: 9780207

33. Vila-Coro AJ, Rodriguez-Frade JM, Martin De Ana A, Moreno-Ortiz MC, Martinez AC, et al. (1999) The chemokine SDF1-α triggers CXCR4 receptor dimerization and activates the JAK/STAT pathway. FASEB J 13: 1699–1710. PMID: 10506573

34. Rodriguez-Frade JM, Vila-Coro AJ, de Ana AM, Albar JP, Martinez AC, et al. (1999) The chemokine monocyte chemoattractant protein-1 induces functional responses through dimerization of its receptor CCR2. Proc Natl Acad Sci U S A 96: 3628–3633. PMID: 10097088

35. Mellado M, Rodriguez-Frade JM, Vila-Coro AJ, Fernandez S, Martin de Ana A, et al. (2001) Chemokine receptor homo- or heterodimerization activates distinct signaling pathways. EMBO J 20: 2497–2507. PMID: 11350939

36. Levoye A, Balabanian K, Baleux F, Bachelerie F, Lagane B (2009) CXCR7 heterodimerizes with CXCR4 and regulates CXCL12-mediated G protein signaling. Blood 113: 6085–6093. doi: 10.1182/blood-2008-12-196618 PMID: 19380869

37. Decaillot FM, Kazmi MA, Lin Y, Ray-Saha S, Sakmar TP, et al. (2011) CXCR7/CXCR4 heterodimer constitutively recruits β-arrestin to enhance cell migration. J Biol Chem 286: 32188–32197. doi: 10.1074/jbc.M111.277038 PMID: 21730065

38. Wang J, He L, Combs CA, Roderiquez G, Norcross MA (2006) Dimerization of CXCR4 in living malignant cells: control of cell migration by a synthetic peptide that reduces homologous CXCR4 interactions. Mol Cancer Ther 5: 2474–2483. PMID: 17041091

39. Hernanz-Falcon P, Rodriguez-Frade JM, Serrano A, Juan D, del Sol A, et al. (2004) Identification of amino acid residues crucial for chemokine receptor dimerization. Nat Immunol 5: 216–223. PMID: 14716309

40. Tenner-Racz K, Racz P, Schmidt H, Dietrich M, Kern P, et al. (1988) Immunohistochemical, electron microscopic and in situ hybridization evidence for the involvement of lymphatics in the spread of HIV-1. AIDS 2: 299–309. PMID: 3140835

41. Murooka TT, Deruaz M, Marangoni F, Vrbanac VD, Seung E, et al. (2012) HIV-infected T cells are migratory vehicles for viral dissemination. Nature 490: 283–287. doi: 10.1038/nature11398 PMID: 22854780

42. Bucy RP, Hockett RD, Derdeyn CA, Saag MS, Squires K, et al. (1999) Initial increase in blood CD4+ lymphocytes after HIV antiretroviral therapy reflects redistribution from lymphoid tissues. J Clin Invest 103: 1391–1398. PMID: 10330421

43. Irhimeh MR, Fitton JH, Lowenthal RM (2007) Fucoidan ingestion increases the expression of CXCR4 on human CD34+ cells. Exp Hematol 35: 989–994. PMID: 17533053

44. Klasse PJ, Moore JP (2004) Is there enough gp120 in the body fluids of HIV-1-infected individuals to have biologically significant effects? Virology 323: 1–8. PMID: 15165814

45. Murphy JW, Cho Y, Sachpatzidis A, Fan C, Hodsdon ME, et al. (2007) Structural and functional basis of CXCL12 (stromal cell-derived factor-1α) binding to heparin. J Biol Chem 282: 10018–10027. PMID: 17264079

46. Bozzini S, Falcone V, Conaldi PG, Visai L, Biancone L, et al. (1998) Heparin-binding domain of human fibronectin binds HIV-1 gp120/160 and reduces virus infectivity. J Med Virol 54: 44–53. PMID: 9443108

47. Geijtenbeek TB, Kwon DS, Torensma R, van Vliet SJ, van Duijnhoven GC, et al. (2000) DC-SIGN, a dendritic cell-specific HIV-1-binding protein that enhances trans-infection of T cells. Cell 100: 587–597. PMID: 10721995

48. Shamri R, Grabovsky V, Gauguet JM, Feigelson S, Manevich E, et al. (2005) Lymphocyte arrest requires instantaneous induction of an extended LFA-1 conformation mediated by endothelium-bound chemokines. Nat Immunol 6: 497–506. PMID: 15834409

Arch Virol (2014) 159:1849–1856
DOI 10.1007/s00705-014-2099-y

BRIEF REPORT

Development of T cell lymphoma in HTLV-1 bZIP factor and Tax double transgenic mice

Tiejun Zhao · Yorifumi Satou · Masao Matsuoka

Received: 13 January 2014 / Accepted: 22 April 2014 / Published online: 13 May 2014

Abstract Adult T-cell leukemia (ATL) is an aggressive T-cell malignancy caused by human T-cell leukemia virus type 1 (HTLV-1). ATL cells possess a CD4+ CD25+ phenotype, similar to that of regulatory T cells (Tregs). Tax has been reported to play a crucial role in the leukemogenesis of HTLV-1. The HTLV-1 bZIP factor (HBZ), which is encoded by the minus strand of the viral genomic RNA, is expressed in all ATL cases and induces neoplastic and inflammatory disease *in vivo*. To test whether HBZ and Tax are both required for T cell malignancy, we generated HBZ/Tax double transgenic mice in which HBZ and Tax are expressed exclusively in CD4+ T cells. Survival was much reduced in HBZ/Tax double-transgenic mice compared with wild type littermates. Transgenic expression of HBZ and Tax induced skin lesions and T-cell lymphoma in mice, resembling diseases observed in HTLV-1 infected individuals. However, Tax single transgenic mice did not develop major health problems. In addition, memory CD4+ T cells and Foxp3+ Treg cells counts were increased in HBZ/Tax double transgenic mice, and their proliferation was enhanced. There was very little difference between HBZ single and HBZ/Tax double transgenic mice. Taken together, these results show that HBZ, in addition to Tax, plays a critical role in T-cell lymphoma arising from HTLV-1 infection.

Keywords HTLV-1 · HBZ · Tax · Transgenic mice · Lymphoma

Introduction

Human T-cell leukemia virus type1 (HTLV-1) was the first retrovirus proven to be associated with human disease. Infection with HTLV-1 causes adult T-cell leukemia (ATL) [20, 24]. ATL cells possess a CD4+ CD25+ phenotype, similar to that of regulatory T cells (Tregs). Previous report showed that HTLV-1 provirus is detected mainly in CD4+ memory T cells and Treg cells, suggesting that HTLV-1 favors Treg cells and memory T cells *in vivo* [10, 23, 26].

HTLV-1 encodes several regulatory (*tax* and *rex*) and accessory (*p12*, *p13*, and *p30*) genes in the pX region between the *env* gene and the 3′ Long terminal repeat (LTR) [19]. Another gene, the *HTLV-1 bZIP factor* (*HBZ*), is encoded by the minus strand of the HTLV-1 genome [4]. Among the proteins encoded by these genes, Tax and HBZ play critical roles in ATL [5, 16]. Accumulating evidence shows that Tax can immortalize human primary T cells, enhance viral replication and support cellular proliferation [5]. However, the expression of Tax cannot be detected in approximately 60 % of fresh ATL cells because of genetic and epigenetic changes in the HTLV-1 provirus, which indicated that Tax may not be essential for the development of ATL [15]. We reported previously that HBZ is

Electronic supplementary material The online version of this article (doi:10.1007/s00705-014-2099-y) contains supplementary material, which is available to authorized users.

T. Zhao (✉)
College of Chemistry and Life Sciences, Zhejiang Normal University, 688 Yingbin Road, Jinhua 321004, Zhejiang, China
e-mail: tjzhao@zjnu.cn

T. Zhao · Y. Satou · M. Matsuoka
Laboratory of Virus Control, Institute for Virus Research, Kyoto University, Kyoto, Japan

Present Address:
Y. Satou
Priority Organization for Innovation and Excellence, Center for AIDS Research, Kumamoto University, Kumamoto, Japan

consistently expressed in all ATL cells and promotes proliferation of ATL cells [21]. Non-sense mutations of all HTLV-1 genes except HBZ were generated by APOBEC3G (A3G), suggesting that HBZ is indispensable for the growth and survival of HTLV-1 infected cells [3].

It is noteworthy that Tax and HBZ synergistically regulated the viral transcription and cellular signaling pathways in ATL [29]. HBZ suppressed Tax-mediated HTLV-1 viral transcription through interaction with cAMP response element-binding protein (CREB) [12]. Additionally, HBZ selectively inhibited the classical nuclear factor-κB (NF-κB) pathway which was activated by Tax [27]. We reported that HBZ induced the differentiation of Treg cells by activating the transforming growth factor-β (TGF-β) pathway [28]. Contrariwise, three distinct mechanisms by which Tax suppressed TGF-β–mediated signaling were reported [1, 11, 17]. Taken together, we speculated that the complementary effect of Tax and HBZ on regulating signaling pathways may facilitate better survival of HTLV-1 infected cells and help the cancer cells escape immune attack.

To test the effect of synchronous expression of HBZ and Tax on T cell malignancy in vivo, we generated double transgenic mice expressing HBZ and Tax under the control of the CD4 promoter. In the present study, we found that HBZ/Tax mice have increased memory CD4+ T cells and Foxp3+ Treg cells, resulting in the development of skin lesions and T-cell lymphoma. Both the skin lesions and the lymphoma resemble diseases observed in HTLV-1 infected individuals.

Material and methods

Mice and cell cultures

C57BL/6 J mice were purchased from CLEA Japan. Transgenic HBZ mice expressing HBZ specifically in CD4+ cells have been described elsewhere [22, 25]. Tax single transgenic mice were generated as previously reported [22]. Male HBZ transgenic mice were mated with female Tax transgenic mice, and offspring were typed for the presence of each transgene. Wild-type, HBZ, and Tax single transgenic mice were maintained as controls along with experimental HBZ/Tax transgenic offspring.

All animal experimentation was performed in strict accordance with the Japanese animal welfare bodies, and the Regulation on Animal Experimentation at Kyoto University. The protocol was approved by the Institutional Animal Research Committees of Kyoto University and Zhejiang Normal University. All efforts were made to minimize suffering.

ATL cell lines, ATL-43T and MT-1, were cultured in RPMI-1640 containing 10 % FBS and antibiotics. 293FT cells were maintained as described previously [27].

Semiquantitative RT-PCR and real-time PCR

Total RNA was isolated using Trizol Reagent (Invitrogen) according to the manufacturer's instructions. We reverse-transcribed total RNA into single-stranded cDNA with SuperScript III reverse transcriptase (Invitrogen). For semiquantitative PCR, cDNA was amplified by increasing PCR cycles using forward (F) and reverse (R) primers specific to the target genes. The expression of transgenic genes was quantified by real-time PCR using the Taqman Universal PCR Master Mix (PE Applied Biosystems) according to the manufacturer's instructions.

Lentiviral vector construction and transfection of recombinant lentivirus

We cloned Tax cDNA into a lentiviral vector, pCSII-EF-MCS. Recombinant lentivirus was produced as described. ATL-43T cells were incubated with concentrated vector stocks in the presence of 4 μg/mL polybrene.

Cell isolation and flow cytometric analysis

Murine spleen was carefully crushed to release the lymphocytes. Splenic erythrocytes were eliminated with NH_4Cl. Cells were washed with PBS containing 1 % FBS. After centrifugation, cells were incubated with antibodies for 30 min at 4 °C, and then analyzed with a flow cytometer (BD FACSCanto II, BD Biosciences). For intracellular staining, we used a mouse Foxp3 staining kit according to its protocol (eBioscience).

BrdU staining

In vivo proliferation was measured by BrdU incorporation. BrdU (Nacalai Tesque) was dissolved in PBS (3 μg/ml), and then 200 μl was injected intraperitoneally into transgenic and non-transgenic mice twice a day for three days. BrdU incorporation in CD4+ splenocytes was detected using FITC BrdU Flow Kits (BD Pharmingen) according to the manufacturer's instructions.

Statistical analysis

Statistical analyses were performed using the unpaired student *t* test.

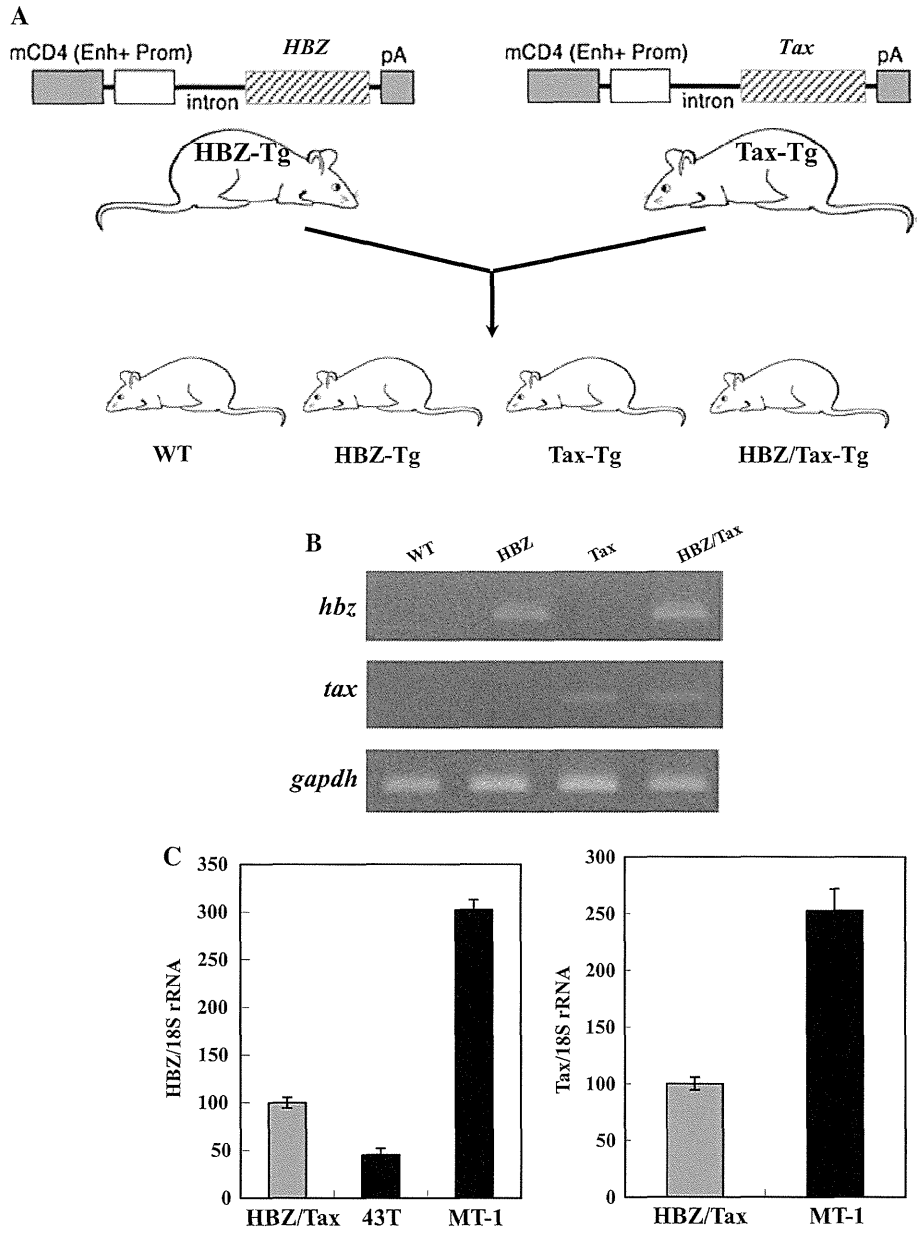

Fig. 1 Generation of HBZ/Tax transgenic (Tg) mice. (A) Schematic representation of the HBZ and Tax transgene. The promoter (Prom) and enhancer (Enh) of the mouse CD4 (mCD4) gene were ligated to HBZ and Tax cDNA plus the polyadenylation signal sequence of SV40. (B) Expression of HBZ and Tax transcripts was detected by RT-PCR in purified CD4+ splenocytes from transgenic mice. (C) Transcripts of the HBZ and Tax genes in CD4+ splenocyte from HBZ/Tax-transgenic mice or ATL cell lines were quantified by real time PCR. ATL-43T and MT-1 are derived from ATL cells

Results

In the development of ATL, Tax is thought to play critical role in leukemogenesis because of its pleiotropic functions [5]. HBZ was constitutively expressed in all ATL cases, and involved in cell proliferation [21]. Additionally, HBZ modulated Tax-mediated viral gene transcription and cellular signaling, suggesting that HBZ cooperates closely with Tax in ATL [2, 7, 12–14, 27, 28]. However, the relevance to T cell malignancy of combined up-regulation of Tax and HBZ has not been established. Since HTLV-1 mainly infects CD4+ T cells, we generated transgenic mice expressing HBZ and Tax under the control of the murine CD4-specific promoter/enhancer/silencer. To test whether HBZ and Tax could cooperate in the development of T cell malignancies, we took advantage of the availability of HBZ and Tax transgenic mice and produced double-transgenic mice expressing both HBZ and Tax in T lymphocytes (Fig. 1A). As shown in Fig. 1B, HBZ and Tax transgene expression was detected by RT-PCR by using CD4+ splenocytes from age-matched mice of the different genotypes. Moreover, HBZ did not interfere with the expression of Tax in double transgenic mice. As shown in Figure 1C, the expression level of HBZ and Tax in transgenic mice was similar to that of ATL cell lines.

Tax single transgenic mice did not develop major health problems, and had a normal life span, as shown in Fig. 2A. In contrast, survival of HBZ and HBZ/Tax double

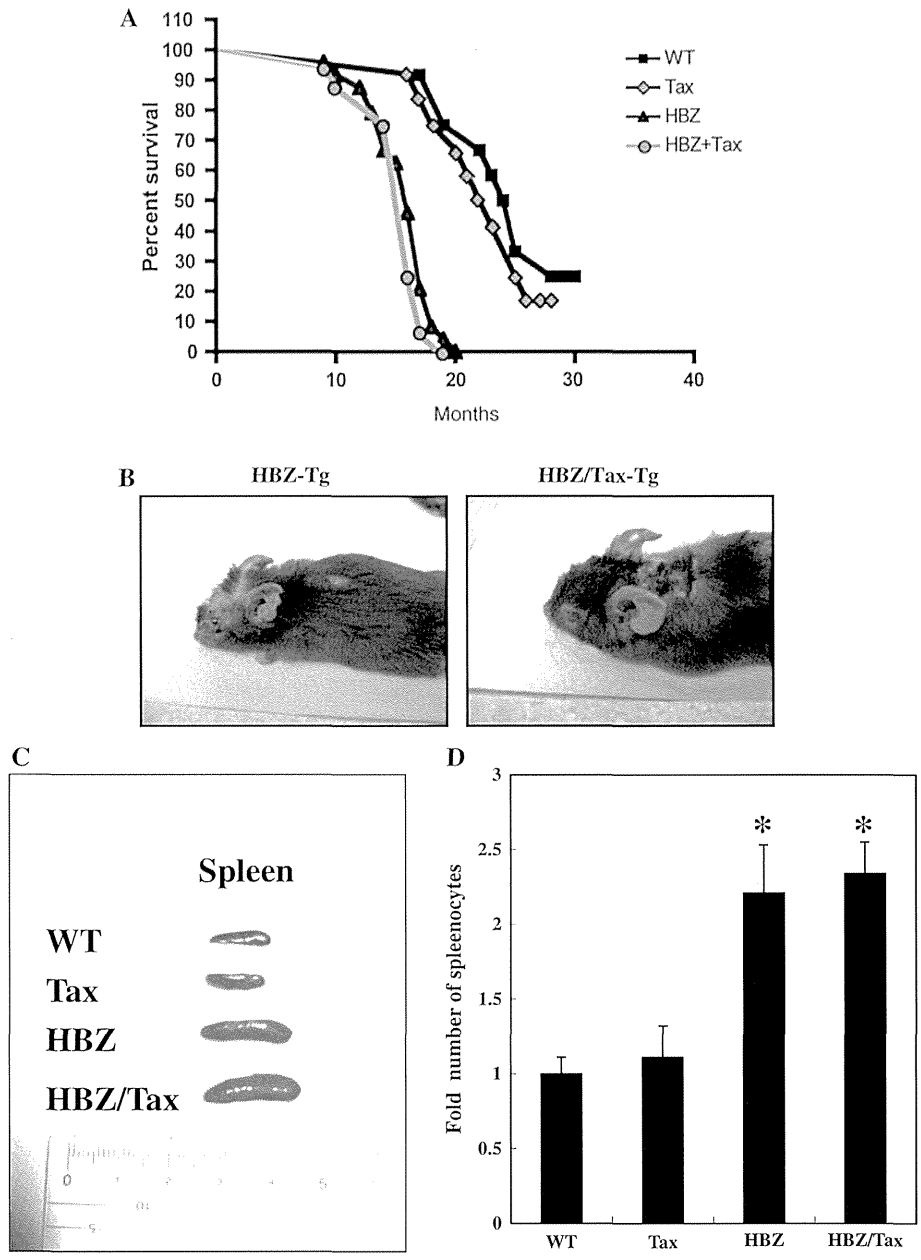

Fig. 2 Characterization of transgenic mice. (A) Kaplan–Meier analysis of survival of wild-type, HBZ single-, Tax single-, and HBZ/Tax double transgenic mice. (B) An HBZ-transgenic and HBZ/Tax mouse with typical skin symptom. (C) Representative examples of spleens from age-matched transgenic mice. (D) Total number of splenocytes of transgenic mice are compared.*, $P < 0.05$ when transgenic mice are compared with wild type littermates by unpaired t test

transgenic mice was much reduced. Some of these mice died as early as ten months after birth. By 20 months, <5% of the HBZ and HBZ/Tax mice remained alive. Interestingly, there is not much difference in survival time between HBZ single transgenic mice and HBZ/Tax double transgenic mice.

Consistent with previous reports, HBZ transgenic mice developed skin lesions by 4 months of age, non-transgenic littermates developed no disease. As shown in Fig. 2B, HBZ/Tax double transgenic mice had similar skin symptoms as HBZ transgenic mice. In Tax transgenic mice, we did not observe inflammatory lesions in the skin (data not shown). Analysis of spleen size in transgenic mice expressing HBZ or Tax alone or in combination revealed splenomegaly in HBZ and HBZ/Tax lines, while tax transgenic mice present spleens of normal size. Moreover, age-matched HBZ/Tax double-transgenic mice had spleens similar in size and weight to HBZ single transgenic mice. Representative examples of the spleens from the various transgenic mice are shown in Fig. 2C. Next, we analyzed the total number of splenic CD4+ T cells in each transgenic line. As shown in Fig. 2D, HBZ and HBZ/Tax mice had, on average, twice the CD4+ splenocytes of wild-type littermates, whereas Tax mice had equal numbers of splenocytes as non-transgenic mice.

Table 1 The incidence of lymphoma in transgenic mice

	WT	Tax-Tg	HBZ-Tg	HBZ/Tax-Tg
Total	52	42	43	32
Lymphoma	2.7 %	2.2 %	32.2 %	34.7 %

The total number of mice and percentage of transgenic mice with lymphoma are listed

Analogous to the incidence of ATL in humans, 32.2 % of HBZ transgenic mice developed T-cell lymphomas after 14 months, in contrast with 2.7 % of non-transgenic mice. As shown in Table 1, the incidence of T-cell lymphomas in HBZ/Tax double transgenic mice is similar to that in HBZ transgenic mice. On the other hand, excessive Tax gene expression did not induce T-cell lymphoma in Tax transgenic mice.

To study the cellular basis of lymphomagenesis in HBZ/Tax double transgenic mice, we next analyzed the phenotype and FoxP3 expression in three month old mice before they developed pathological manifestations. A previous report showed that effector/memory and CD4+ FoxP3+ regulatory T cells were increased in the HBZ-transgenic mice [22]. We found in this study that the percentage of CD4 single positive T cells increased in the HBZ/Tax transgenic mice (Fig. 3). Moreover, transgenic expression of Tax and HBZ induced Foxp3 expression. We also observed an increased population of effector/memory T cells in the HBZ/Tax transgenic mice, yet the percentage of effector/memory T cells or Treg cells in the Tax-transgenic mice did not change significantly. In addition, there is not much difference in the enhancement of memory and FoxP3+ CD4+ regulatory T-cell populations between HBZ and HBZ/Tax transgenic mice. Taken together, these observations demonstrate that HBZ increased memory T cells and Foxp3 induction in CD4+ T cells regardless of Tax.

We further studied whether Tax has any influence on the generation of Foxp3+ T cells *in vivo*. As shown in Supplemental Fig. 1, retrovirally expressed Tax protein could not increase the level of Foxp3 in ATL-43T, an HTLV-1-associated cell line, which does not express Foxp3.

To study the growth-promoting activity of the HBZ and Tax genes, we assessed the proliferation of CD4+ T cells in transgenic mice by incorporation of BrdU. We found that, in HBZ and HBZ/Tax transgenic mice, the proliferation of CD4+ T cells was three fold-higher than in non-transgenic mice, whereas the proliferation of CD4+ T cells of Tax transgenic mice was similar to that in non-transgenic mice (Fig. 4).

All of these results suggest an important role for HBZ, in addition to Tax, in the oncogenic activity of HTLV-1.

Discussion

Over the past 35 years, substantial effort has been made toward investigating the HTLV-1 associated viral proteins and their regulatory functions [15]. Tax has been shown to be a viral oncogene, since it transforms and immortalizes rodent cells and human T-lymphocytes [15]. HBZ is the only viral gene which is conserved and expressed in all ATL cases, indicating that HBZ is indispensable for HTLV-1 infection and development of ATL [16]. Accumulating evidences shows that HBZ and Tax synergistically dysregulate cell signaling pathways in ATL and determine the cell fate, despite the fact that HBZ and Tax have opposite effects on regulation of cellular activity [2, 13, 14, 27, 28]. For example, HBZ was found to inhibit the Tax-mediated transactivation of viral transcription from the 5′LTR by interacting with JUN and CREB. HBZ overcame the suppression function of Tax on the TGF-β pathway, leading to the activation of TGF-β signaling and differentiation of Foxp3+ CD4+ regulatory T cells. Thus, we proposed that HTLV-1 may take advantage of the complementary functions of HBZ and Tax to facilitate the onset of ATL. So far, there has been no direct evidence for HBZ and Tax together inducing T cell malignancy in vivo. The present study demonstrated that HBZ/Tax double transgenic mice indeed developed T cell lymphoma and inflammation via increased memory T cells and Treg cells.

Since Tax is the major target of cytotoxic T-lymphocytes (CTLs), host cells have developed several mechanisms to silence the expression of Tax [9]. Tax transcripts are detected in only ~40 % of ATL patients. Therefore, HBZ maintains cell proliferation in the late stage of ATL when Tax expression is lost. In this study, we demonstrated that HBZ/Tax double and HBZ single transgenic mice developed neoplastic and inflammatory diseases, while mice expressing only Tax did not. Thus, we suggest that constitutively expressed HBZ is the predominant driver of leukemogenesis of ATL.

It has been reported that Tax transgenic mice develop tumors [6, 8, 18]. In those reports, the type of tumor induced by Tax depended on the promoter used. In this study, we generated Tax transgenic mice using the CD4-specific promoter/enhancer/silencer which has previously been used in generating HBZ-transgenic mice. The Tax transgenic mice thus generated did not show any change in the number of Foxp3+ Treg cells or memory T cells, in contrast to mice expressing HBZ, who developed T cell lymphomas. Moreover, since there was no difference in disease between HBZ single and HBZ/Tax double transgenic mice, expression of Tax did not synergistically enhance the lymphomagenesis by HBZ. These data

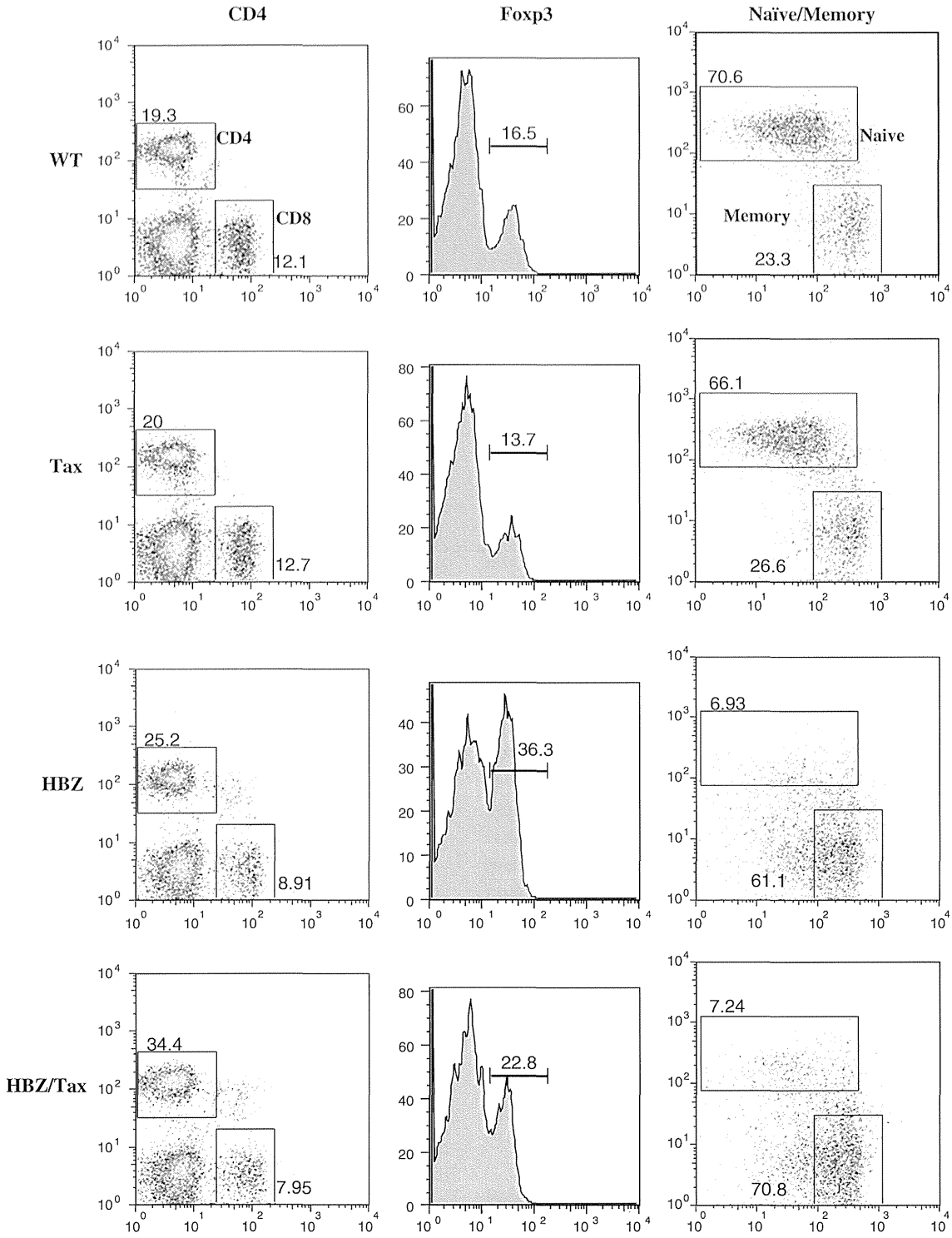

Fig. 3 Transgenic expression of HBZ/Tax in CD4+ T cells increases Foxp3+ Treg and memory T cells. Mouse splenocytes were stained with the indicated antibodies, and analyzed by flow cytometry. Representative dot plots gated on the CD4+ population are shown. For these experiments, HBZ and HBZ/Tax transgenic mice without any symptoms were used

suggest that HBZ, rather than Tax, is responsible for conferring the specific phenotype of HTLV-1 infected cells, and for triggering the development of ATL.

In conclusion, we showed that HBZ single and HBZ/Tax double transgenic mice spontaneously develop T cell lymphomas and inflammatory diseases similar to those in

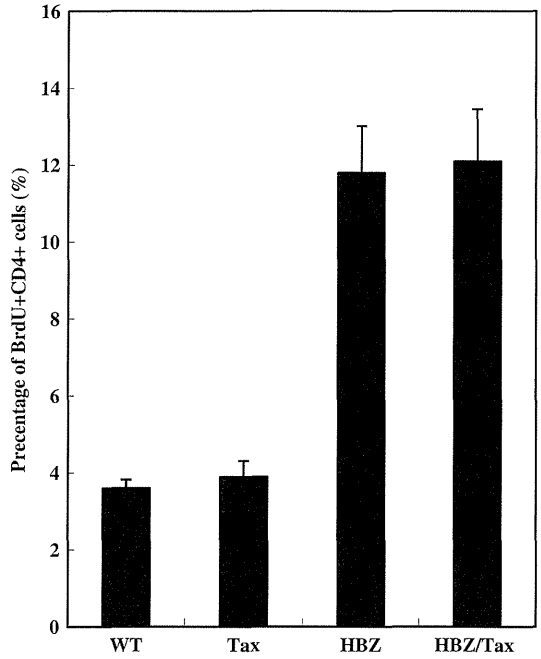

Fig. 4 CD4+ T cells proliferated in HBZ/Tax transgenic mice. BrdU was injected into mice twice a day for three days, and splenocytes were stained with antibodies to BrdU and CD4

HTLV-1 infected individuals. However, Tax single transgenic mice did not develop major health problems. This study highlights the importance of HBZ in HTLV-1-associated disease.

Acknowledgments This work was supported by a grant from National Natural Science Foundation of China to TZ (No.31200128); a Grant-in-aid for Scientific Research from the Ministry of Education, Science, Sports, and Culture of Japan to MM. The authors thank Aaron Coutts for proofreading the manuscript.

Conflict of interest The authors declare that they have no competing interests.

References

1. Arnulf B, Villemain A, Nicot C, Mordelet E, Charneau P, Kersual J, Zermati Y, Mauviel A, Bazarbachi A, Hermine O (2002) Human T-cell lymphotropic virus oncoprotein Tax represses TGF-beta 1 signaling in human T cells via c-Jun activation: a potential mechanism of HTLV-I leukemogenesis. Blood 100:4129–4138
2. Basbous J, Arpin C, Gaudray G, Piechaczyk M, Devaux C, Mesnard JM (2003) The HBZ factor of human T-cell leukemia virus type I dimerizes with transcription factors JunB and c-Jun and modulates their transcriptional activity. J Biol Chem 278:43620–43627
3. Fan J, Ma G, Nosaka K, Tanabe J, Satou Y, Koito A, Wain-Hobson S, Vartanian JP, Matsuoka M (2010) APOBEC3G generates nonsense mutations in human T-cell leukemia virus type 1 proviral genomes in vivo. J Virol 84:7278–7287
4. Gaudray G, Gachon F, Basbous J, Biard-Piechaczyk M, Devaux C, Mesnard JM (2002) The complementary strand of the human T-cell leukemia virus type 1 RNA genome encodes a bZIP transcription factor that down-regulates viral transcription. J Virol 76:12813–12822
5. Grassmann R, Aboud M, Jeang KT (2005) Molecular mechanisms of cellular transformation by HTLV-1 Tax. Oncogene 24:5976–5985
6. Grossman WJ, Kimata JT, Wong FH, Zutter M, Ley TJ, Ratner L (1995) Development of leukemia in mice transgenic for the tax gene of human T-cell leukemia virus type I. Proc Natl Acad Sci USA 92:1057–1061
7. Hagiya K, Yasunaga J, Satou Y, Ohshima K, Matsuoka M (2011) ATF3, an HTLV-1 bZip factor binding protein, promotes proliferation of adult T-cell leukemia cells. Retrovirology 8:19
8. Hasegawa H, Sawa H, Lewis MJ, Orba Y, Sheehy N, Yamamoto Y, Ichinohe T, Tsunetsugu-Yokota Y, Katano H, Takahashi H, Matsuda J, Sata T, Kurata T, Nagashima K, Hall WW (2006) Thymus-derived leukemia-lymphoma in mice transgenic for the Tax gene of human T-lymphotropic virus type I. Nat Med 12:466–472
9. Kannagi M, Harada S, Maruyama I, Inoko H, Igarashi H, Kuwashima G, Sato S, Morita M, Kidokoro M, Sugimoto M et al (1991) Predominant recognition of human T cell leukemia virus type I (HTLV-I) pX gene products by human CD8+ cytotoxic T cells directed against HTLV-I-infected cells. Int Immunol 3:761–767
10. Karube K, Ohshima K, Tsuchiya T, Yamaguchi T, Kawano R, Suzumiya J, Utsunomiya A, Harada M, Kikuchi M (2004) Expression of FoxP3, a key molecule in CD4CD25 regulatory T cells, in adult T-cell leukaemia/lymphoma cells. Br J Haematol 126:81–84
11. Lee DK, Kim BC, Brady JN, Jeang KT, Kim SJ (2002) Human T-cell lymphotropic virus type 1 tax inhibits transforming growth factor-beta signaling by blocking the association of Smad proteins with Smad-binding element. J Biol Chem 277:33766–33775
12. Lemasson I, Lewis MR, Polakowski N, Hivin P, Cavanagh MH, Thebault S, Barbeau B, Nyborg JK, Mesnard JM (2007) Human T-cell leukemia virus type 1 (HTLV-1) bZIP protein interacts with the cellular transcription factor CREB to inhibit HTLV-1 transcription. J Virol 81:1543–1553
13. Ma G, Yasunaga J, Fan J, Yanagawa S, Matsuoka M (2012) HTLV-1 bZIP factor dysregulates the Wnt pathways to support proliferation and migration of adult T-cell leukemia cells. Oncogene 32:4222–4230
14. Matsumoto J, Ohshima T, Isono O, Shimotohno K (2005) HTLV-1 HBZ suppresses AP-1 activity by impairing both the DNA-binding ability and the stability of c-Jun protein. Oncogene 24:1001–1010
15. Matsuoka M, Jeang KT (2007) Human T-cell leukaemia virus type 1 (HTLV-1) infectivity and cellular transformation. Nat Rev Cancer 7:270–280
16. Matsuoka M, Green PL (2009) The HBZ gene, a key player in HTLV-1 pathogenesis. Retrovirology 6:71
17. Mori N, Morishita M, Tsukazaki T, Giam CZ, Kumatori A, Tanaka Y, Yamamoto N (2001) Human T-cell leukemia virus type I oncoprotein Tax represses Smad-dependent transforming growth factor beta signaling through interaction with CREB-binding protein/p300. Blood 97:2137–2144
18. Nerenberg M, Hinrichs SH, Reynolds RK, Khoury G, Jay G (1987) The tat gene of human T-lymphotropic virus type 1 induces mesenchymal tumors in transgenic mice. Science 237:1324–1329
19. Nicot C, Harrod RL, Ciminale V, Franchini G (2005) Human T-cell leukemia/lymphoma virus type 1 nonstructural genes and their functions. Oncogene 24:6026–6034

20. Poiesz BJ, Ruscetti FW, Gazdar AF, Bunn PA, Minna JD, Gallo RC (1980) Detection and isolation of type C retrovirus particles from fresh and cultured lymphocytes of a patient with cutaneous T-cell lymphoma. Proc Natl Acad Sci USA 77:7415–7419
21. Satou Y, Yasunaga J, Yoshida M, Matsuoka M (2006) HTLV-I basic leucine zipper factor gene mRNA supports proliferation of adult T cell leukemia cells. Proc Natl Acad Sci USA 103:720–725
22. Satou Y, Yasunaga J, Zhao T, Yoshida M, Miyazato P, Takai K, Shimizu K, Ohshima K, Green PL, Ohkura N, Yamaguchi T, Ono M, Sakaguchi S, Matsuoka M (2011) HTLV-1 bZIP factor induces T-cell lymphoma and systemic inflammation in vivo. Plos Pathogens 7:e1001274
23. Toulza F, Heaps A, Tanaka Y, Taylor GP, Bangham CR (2008) High frequency of CD4+ FoxP3+ cells in HTLV-1 infection: inverse correlation with HTLV-1-specific CTL response. Blood 111:5047–5053
24. Uchiyama T, Yodoi J, Sagawa K, Takatsuki K, Uchino H (1977) Adult T-cell leukemia: clinical and hematologic features of 16 cases. Blood 50:481–492
25. Yamamoto-Taguchi N, Satou Y, Miyazato P, Ohshima K, Nakagawa M, Katagiri K, Kinashi T, Matsuoka M (2013) HTLV-1 bZIP Factor Induces Inflammation through Labile Foxp3 Expression. Plos Pathogens 9:e1003630
26. Yamano Y, Takenouchi N, Li HC, Tomaru U, Yao K, Grant CW, Maric DA, Jacobson S (2005) Virus-induced dysfunction of CD4 + CD25 + T cells in patients with HTLV-I-associated neuroimmunological disease. J Clin Invest 115:1361–1368
27. Zhao T, Yasunaga J, Satou Y, Nakao M, Takahashi M, Fujii M, Matsuoka M (2009) Human T-cell leukemia virus type 1 bZIP factor selectively suppresses the classical pathway of NF-kappaB. Blood 113:2755–2764
28. Zhao T, Satou Y, Sugata K, Miyazato P, Green PL, Imamura T, Matsuoka M (2011) HTLV-1 bZIP factor enhances TGF-beta signaling through p300 coactivator. Blood 118:1865–1876
29. Zhao T, Matsuoka M (2012) HBZ and its roles in HTLV-1 oncogenesis. Front Microbiol 3:247

OPEN ACCESS Freely available online

PLOS | ONE

Phylodynamic Analysis Reveals CRF01_AE Dissemination between Japan and Neighboring Asian Countries and the Role of Intravenous Drug Use in Transmission

Teiichiro Shiino[1], Junko Hattori[2], Yoshiyuki Yokomaku[2], Yasumasa Iwatani[2,3], Wataru Sugiura[2,3]*, Japanese Drug Resistance HIV-1 Surveillance Network[¶]

1 Infectious Disease Surveillance Center, National Institute of Infectious Diseases, Tokyo, Japan, **2** Department of Infectious Diseases and Immunology, Clinical Research Center, Nagoya Medical Center, Nagoya, Japan, **3** Department of AIDS Research, Nagoya University Graduate School of Medicine, Nagoya, Japan

Abstract

Background: One major circulating HIV-1 subtype in Southeast Asian countries is CRF01_AE, but little is known about its epidemiology in Japan. We conducted a molecular phylodynamic study of patients newly diagnosed with CRF01_AE from 2003 to 2010.

Methods: Plasma samples from patients registered in Japanese Drug Resistance HIV-1 Surveillance Network were analyzed for protease-reverse transcriptase sequences; all sequences undergo subtyping and phylogenetic analysis using distance-matrix-based, maximum likelihood and Bayesian coalescent Markov Chain Monte Carlo (MCMC) phylogenetic inferences. Transmission clusters were identified using interior branch test and depth-first searches for sub-tree partitions. Times of most recent common ancestor (tMRCAs) of significant clusters were estimated using Bayesian MCMC analysis.

Results: Among 3618 patient registered in our network, 243 were infected with CRF01_AE. The majority of individuals with CRF01_AE were Japanese, predominantly male, and reported heterosexual contact as their risk factor. We found 5 large clusters with ≥5 members and 25 small clusters consisting of pairs of individuals with highly related CRF01_AE strains. The earliest cluster showed a tMRCA of 1996, and consisted of individuals with their known risk as heterosexual contacts. The other four large clusters showed later tMRCAs between 2000 and 2002 with members including intravenous drug users (IVDU) and non-Japanese, but not men who have sex with men (MSM). In contrast, small clusters included a high frequency of individuals reporting MSM risk factors. Phylogenetic analysis also showed that some individuals infected with HIV strains spread in East and South-eastern Asian countries.

Conclusions: Introduction of CRF01_AE viruses into Japan is estimated to have occurred in the 1990s. CFR01_AE spread via heterosexual behavior, then among persons connected with non-Japanese, IVDU, and MSM. Phylogenetic analysis demonstrated that some viral variants are largely restricted to Japan, while others have a broad geographic distribution.

Citation: Shiino T, Hattori J, Yokomaku Y, Iwatani Y, Sugiura W, et al. (2014) Phylodynamic Analysis Reveals CRF01_AE Dissemination between Japan and Neighboring Asian Countries and the Role of Intravenous Drug Use in Transmission. PLoS ONE 9(7): e102633. doi:10.1371/journal.pone.0102633

Editor: Yury E. Khudyakov, Centers for Disease Control and Prevention, United States of America

Received November 23, 2013; **Accepted** June 21, 2014; **Published** July 15, 2014

Funding: This work was supported by a Grant-in-Aid for AIDS research from the Ministry of Health, Labour, and Welfare of Japan [H22-AIDS-004]. The funders had no role in study design, data collection and analysis, decision to publish, or preparation of the manuscript.

Competing Interests: The authors have declared that no competing interests exist.

* Email: wsugiura@nnh.hosp.go.jp

¶ Membership of the Japanese Drug Resistance HIV-1 Surveillance Network is provided in the Acknowledgments.

Introduction

Since the first HIV-1-infected case was identified in Japan in 1985, the cumulative number of reported cases of HIV/AIDS has been increasing every year, reaching 18,447 by the end of 2010 [1]. The major HIV-1 subtype in the 1980s in Japan was subtype B [2] followed by CRF01_AE [3]. CRF01_AE caused an outbreak among the high-risk heterosexual population in Thailand in the late 1980s [4–6], and was subsequently disseminated to various risk populations in neighboring countries, including Vietnam, Cambodia, Malaysia, Indonesia and China [7–15]. Overall the CRF01_AE is substantial, accounting for an estimated 36% of HIV in South, Southeast, and East Asia (Los Alamos database) in CRF01_AE was likely introduced into Japan's heterosexual population in the early phase of the epidemic [3,4,7], but the characteristics of the spread of CRF01_AE in Japan have not been extensively investigated. Our surveillance research showed that from 2003 to 2008 CRF01_AE was the second most prevalent subtype (8.4%) after subtype B, and its host characteristics are distinct from those of the subtype B population [16]. CRF01_AE cases are significantly linked to heterosexual transmission [3,16,17] and non-Japanese people [16]. In contrast, subtype B tends to be found in men who have sex with men (MSM) and Japanese people.

CRF01_AE cases appear to be diagnosed in Japan at a later stage of infection [16], and trends in the CRF01_AE epidemic in Japan have been difficult to study by conventional descriptive epidemiological methods. However, recent advances in computational science have allowed us to infer the evolutionary dynamics

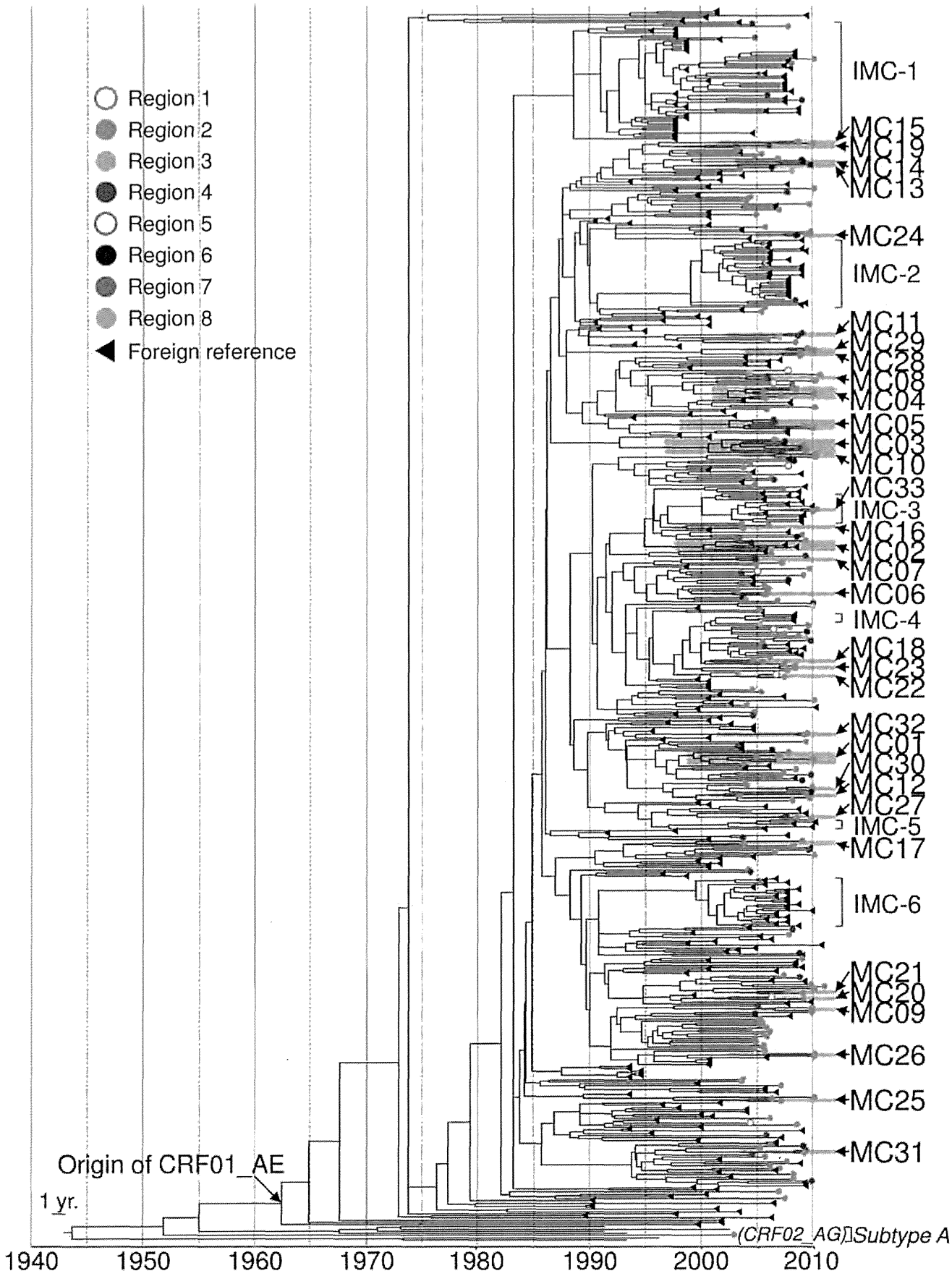
Region 1
Region 2
Region 3
Region 4
Region 5
Region 6
Region 7
Region 8
Foreign reference
IMC-1
MC15
MC19
MC14
MC13
MC24
IMC-2
MC11
MC29
MC28
MC08
MC04
MC05
MC03
MC10
MC33
IMC-3
MC16
MC02
MC07
MC06
IMC-4
MC18
MC23
MC22
MC32
MC01
MC30
MC12
MC27
IMC-5
MC17
IMC-6
MC21
MC20
MC09
MC26
MC25
MC31
Origin of CRF01_AE
1 yr.
(CRF02_AG)Subtype A
1940
1950
1960
1970
1980
1990
2000
2010

Figure 1. Maximum clade credibility tree for partial *pol* region identifies 33 micro-clades within CRF01_AE cases in Japan. Phylodynamic Analysis. The branch length of the phylogeny is in units of time. Patient sequences obtained from surveillance are designated by open or solid circles. Circle color indicates geographic origin of the samples in Japan. Reference sequences from the Los Alamos HIV database are designated by black triangles. Micro-clades (MC) are annotated by red shading and international micro-clades (IMC) are marked with red brackets on the right of the tree.
doi:10.1371/journal.pone.0102633.g001

of a pathogen population from large-scale sequence data using methods, now referred to as "phylodynamics" [18]. Phylodynamics has been used to aid in the analysis of spread of infectious agents with a rapid evolutionary rate [18], e.g., RNA viruses including influenza A [19–21], hepatitis C [22,23], and HIV-1 [24–26]. Since 2003, we have been collecting HIV-1 nucleotide sequence data from newly diagnosed patients in Japan as part of our nationwide surveillance project [16,27]. Here we report our results from applying the phylodynamics approach to these sequence data to understand trends in the CRF01_AE outbreak in Japan, genetic relationships between the circulating strains within Japan and strains observed in the surrounding Asian countries, details of their transmission risk factors, and finally to identify the target populations for effective action plans to prevent further transmission of CRF01_AE.

Materials and Methods

Ethical Statement

This study was conducted according to principles in the Declaration of Helsinki. The study was approved by the human subject research committee at the National Institute of Infectious Diseases and Nagoya Medical Center, Japan. All patients provided written informed consent for the collection of samples and subsequent analyses.

Sample Collection and Viral Gene Sequences

Viral samples were collected from HIV-1-infected patients newly diagnosed from January 2003 to March 2010 at 30 clinics and public health centers in Japan that have participated in our Japanese Drug Resistance HIV-1 Surveillance Network [16,27]. These collection areas are classified into 8 regions according to the nationwide systemic network of hospitals in Japan [28] (Figure S1). The study sample comprised 3618 individuals both acutely and chronically infected. At diagnosis or the earliest hospital visit, patients' peripheral blood was drawn into a vacutainer with EDTA added. At the same time, demographic information was collected on age, gender, nationality, and risk behavior. Plasma samples were analyzed for the nucleotide sequences of HIV-1 protease and the 1- to 240-amino acid region of reverse-transcriptase (RT) using the direct sequencing method of RT-PCR products, and the HIV-1 subtype was determined using phylogenetic analysis as reported [16,27]. This analysis showed that 243 individuals were infected with CRF01_AE at least in the protease-RT regions. GenBank accession numbers of the nucleotide sequences are AB356098–AB556499, AB44228–AB442360, and AB863746–AB871315.

Sequence Alignment of Reconstructed Variants

Direct sequence data may contain loci with multiple peaks, including drug-resistance mutation sites. As these ambiguous loci are generally excluded from analysis by phylogenetic programs, and we wanted to use collected sequences to the maximum in further analyses, we separated these multiple nucleotides into individual nucleotides and reconstructed hypothetical sequence variants possessing each nucleotide as follows. Briefly, protease and RT sequences were concatenated and aligned using Clustal W, version 2.0.10 [29]. Then, a consensus sequence was calculated for the alignment, and ambiguous nucleotides were classified into two groups: overlapping and non-overlapping ambiguities. The former shows one polymorphic nucleotide shared with the consensus allele, while the latter shows a fixation of different alleles from the consensus one [26]. The consensus allele found in the overlapping site was adopted for the reconstructed sequence, and the non-overlapping site was segregated into two haplotypes that carried each nucleotide of the ambiguous site. Consequently, the total number of reconstructed sequences became 297.

These sequences were realigned with foreign CRF01_AE outlier sequences selected as follows. Since transmission clusters have been developed according to scale-free networks in many infectious agents [24,26,30,31], we calculated a frequency distribution of the cluster scale-free network for our observed population in Japan ($n = 297$) by Barabasi's model of scale-free networks [32]. This calculation used the barabasi.game function in igraph library of R software [33]. We estimated that 32.5% of the sequences should be involved in one cluster. Then, using a one-sided error range and rejection coefficient of 0.025 and 1.96 for within and outside clusters, respectively, we calculated the necessary size of the outlier sequence dataset for even allocations within and outside clusters and out of clusters as greater than 332.1. Based on this estimate, we randomly selected 333 CRF01_AE sequences from 37 countries in five regions (Africa, North America, South America, Asia and Europe) submitted to the Los Alamos HIV database before 2010 and used them as the foreign outlier dataset (Table S1). The sequences were further aligned with the following 6 subtype A outgroup sequences: A1.UG.92.92UG037, A1.KE.94.Q23_17, A1.AU.03.PS1044_Day0, A1.RW.92.92RW008, A2.CD.97.97CDKTB48, and A2.CY.94.94CY017_41. The resulting alignment was corrected by hand for gaps. The reference and outlier sequences were collected from the Los Alamos HIV database (http://www.hiv.lanl.gov/content/index.html). The final number of sites in the aligned sequence was 1150 bases.

Phylogenetic Inferences of the Viral Gene Sequence

To eliminate the influence of antiretroviral drug treatments on viral evolution, we made a codon-stripped sequence alignment by removing 43 drug resistance-associated codons defined in our previous studies [16,27]. This alignment was used to estimate a matrix of the number of substitutions between each sequence pair by the composite likelihood method [34], and to infer the neighbor-joining (NJ) tree with the interior branch test. The sequence alignment was also used to infer the maximum likelihood tree using the same substitution model described below with a bootstrap test of 500 replicates. In this process, one of the 244 subjects preliminarily classified into CRF01_AE was re-classified into CRF02_AG (Figure 1 and Figure S2). We excluded this subject in the following analyses. The distance matrix was also used to calculate the mean number of base substitutions per site (i.e., genetic diversity) within and between arbitrary subpopulations, and the coefficient of differentiation between subpopulations. Standard error estimates for genetic diversity were obtained by a bootstrap test with 500 replicates. The analyses were conducted using MEGA version 5.0 [35].

Table 1. Demographic Characteristics of CRF01_AE HIV-1-Infected Individuals in Japan ($N = 243$).

Characteristic		Male		Female		Unknown	Total	
		n	%	*n*	%	*n*	*n*	%
Nationality								
Japanese		128	52.7	36	14.8	1	165	67.9
Asian countries		19	7.8	31	12.8	0	50	20.6
China		1	0.4	3	1.2	0	4	1.6
Philippines		0	0.0	1	0.4	0	1	0.4
Vietnam		3	1.2	0	0.0	0	3	1.2
Malaysia		2	0.8	0	0.0	0	2	0.8
Indonesia		4	1.6	4	1.6	0	8	3.3
Thailand		5	2.1	19	7.8	0	24	9.9
Laos		1	0.4	1	0.4	0	2	0.8
Myanmar		3	1.2	3	1.2	0	6	2.5
South American countries		1	0.4	1	0.4	0	2	0.8
Brazil		0	0.0	1	0.4	0	1	0.4
Peru		1	0.4	0	0.0	0	1	0.4
Unspecified		4	1.6	2	0.8	0	6	2.5
Unknown		13	5.3	4	1.6	3	20	8.2
Transmission category								
High-risk heterosexual contact		104	42.8	62	25.5	0	166	68.3
Male-to-male sexual contact		37	15.2	NA	NA	0	37	15.2
Intravenous drug user		7	2.9	2	0.8	0	9	3.7
Unidentified		17	6.6	10	4.1	4	31	12.8
Area of clinics and facilities								
Region 1	(Hokkaido)	3	1.2	3	1.2	1	7	2.9
Region 2	(Kanto)	112	46.1	48	19.8	3	163	67.1
Region 3	(Koushinetsu)	4	1.6	4	1.6	0	8	3.3
Region 4	(Tokai)	26	10.7	14	5.7	0	40	16.5
Region 5	(Hokuriku)	1	0.4	1	0.4	0	2	0.8
Region 6	(Kinki)	15	6.2	2	0.8	0	17	7.0
Region 7	(Kyushu)	2	0.8	1	0.4	0	3	1.2
Region 8	(Okinawa)	2	0.8	1	0.4	0	3	1.2
Age, years								
20–29		33	13.6	21	8.6	0	54	22.2
30–39		36	14.8	26	10.7	0	62	25.5
40–49		49	20.2	11	4.5	0	60	24.7

Table 1. Cont.

Characteristic	Male		Female		Unknown	Total	
	n	%	*n*	%	*n*	*n*	%
50–59	26	10.7	8	3.3	0	34	14.0
60–69	20	8.2	7	2.9	0	27	11.1
>70	1	0.4	1	0.4	0	2	0.8
Unknown	0	0	0	0	4	4	1.6
Total	165	67.9	74	30.5	4	243	100

NA: not available.

doi:10.1371/journal.pone.0102633.t001

Phylodynamic Analysis

The best-fit model for nucleotide substitution was evaluated by the hierarchical likelihood ratio test using PAUP v4.0 [36] with MrModeltest [37], and the general time-reversible model was adopted with gamma-distributed site heterogeneity and invariant sites (GTR+G+I) with four rate categories. Evolutionary parameters, chronological maximum clade credibility phylogeny, and the times of the most recent common ancestors (tMRCAs) were estimated from the sequence alignment using the Bayesian Coalescent Markov Chain Monte Carlo (MCMC) approach implemented in BEAST v1.7.4 [38]. The sequence was partitioned into 3-codon positions. To select a model for population growth and the molecular clock, we used Bayesian factor comparison [39] with the marginal likelihood estimated by the stepping-stone sampling method [40,41] using preliminary runs of BEAST with MCMC chains of 100 million iterations. Constant population growth and relaxed clock with an uncorrelated lognormal-distribution was adopted as a best-fit model (Table S2). The best-fit parameters were then used in an additional MCMC analysis consisting of 500 million iterations to estimate the evolutionary parameters. The convergence of parameters was inspected using Tracer v.1.5, with uncertainties depicted as 95% highest probability density (HPD) intervals. The effective sample size of each parameter calculated in this inference was above 200. Tree samples in the MCMC were used to generate a maximum clade credibility tree using TreeAnnotator v.1.5.4 with a burn-in of 40000 states.

Identification of Endemic Transmission Clusters

To identify viral transmission clusters, we performed three analyses; those matching all three approaches were recognized as monophyletic groups. The first approach was to evaluate the reliability of tree topology. We selected transmission cluster candidates from identical tree clusters with three different inference methods: NJ, maximum likelihood and maximum clade credibility tree in Bayesian MCMC. The second approach was a test of monophyly using the interior branch test in NJ tree and a posterior probability in Bayesian MCMC, in which significant clusters were determined as having $\geq$95% confidence probability for a target cluster. The third approach considered genetic divergence of the cluster against the whole sequence diversity. The distributions of all pairwise distances in the given phylogeny were calculated, and a specific sub-tree was then identified as a micro-clade if the median value of genetic distance between each pair of sub-tree members was lower than a threshold, determined as the 10^{th} percentile density (median diversity limit being 0.026) [42]. After a depth-first search of a rooted tree with all three approaches, small groups of viruses with clear evidence of common ancestry (posterior probability $\geq$0.95 in Baysian MCMC inference) were detected; we denoted these groups as "micro-clades", as previously described for small groupings of circulating viral variants viruses [21]. Micro-clades were classified in two groups according to their origins; one is a cluster group having its ancestral virus from Japan (domestic micro-clade), and the other is a cluster group having its ancestral virus from foreign countries (international micro-clade). Micro-clades were then classified as transmission clusters with three or more cases, and cluster candidates as heterosexual, MSM or intravenous drug user (IVDU) pairs. The depth-first search of the clusters was computed by in-house scripts written in Perl 5. The tMRCA was estimated for each domestic micro-clade.